Mathematical Modelling and Numerical Analysis Will be set by the publisher
Modélisation Mathématique et Analyse Numérique

RESIDUAL BASED AND HIERARCHICAL A POSTERIORI ERROR ESTIMATES FOR NONCONFORMING MIXED FINITE ELEMENT METHODS

Linda El Alaoui[1] and Alexandre Ern[1]

Abstract. We consider nonconforming mixed finite element approximations to elliptic problems with variable coefficients, arising for instance in the modeling of Darcy flows through heterogeneous porous media. We investigate two types of a posteriori error indicators based on either local residuals or a two-level hierarchical setting. We prove that all the estimators yield upper and lower bounds for the numerical error. Finally, we present numerical results illustrating the efficiency of the estimators.

Résumé. Nous considérons des approximations numériques par éléments finis mixtes non-conformes de problèmes elliptiques à coefficients variables, comme ceux rencontrés par exemple dans la modélisation d'écoulements darcéens en milieu poreux hétérogène. Nous étudions des indicateurs d'erreur a posteriori de type résidu et de type hiérarchique. Nous montrons que ces estimateurs bornent inférieurement et supérieurement l'erreur numérique. Nous présentons enfin des résultats numériques illustrant l'efficacité de ces estimateurs.

1991 Mathematics Subject Classification. 65N60, 65N15, 75N12, 76905.

The dates will be set by the publisher.

1. Introduction

The main motivation for this work is the numerical simulation of subsurface flows in saturated porous media. In such simulations, it is often critical to achieve highly accurate flow velocity predictions in order to investigate pollutant transfer by advective, diffusive and dispersive effects. A widely used physical model for steady subsurface flows in saturated porous media consists of Darcy equations

$$\begin{cases} j + k\nabla u = 0\,, \\ \nabla\cdot j = f\,, \end{cases} \tag{1.1}$$

where j is the velocity vector, k the hydraulic conductivity, u the hydraulic head (or the pressure up to an appropriate rescaling) and f the source term resulting from mass sources or sinks. The first equation in (1.1) is Darcy's phenomenological law and the second equation expresses mass conservation. Problem (1.1) is posed on the computational domain Ω and is completed by flux or head conditions on the boundary $\partial\Omega$. Elimination

Keywords and phrases: Finite elements, Petrov-Galerkin method, Nonconforming methods, A posteriori error estimates, Darcy equations, Heterogeneous media

[1] CERMICS, Ecole nationale des ponts et chaussées, 6 et 8, avenue Blaise Pascal, F-77455 Marne la Vallée cedex 2, France ; e-mail: `{elalaoui,ern}@cermics.enpc.fr`

of the velocity unknown yields the elliptic equation

$$-\nabla \cdot (k \nabla u) = f\,. \tag{1.2}$$

Equations (1.1) and (1.2) arise in many other models, the former providing a mixed formulation of the latter.

Problem (1.1) may be cast into several weak formulations. On the one hand, one may consider two symmetric formulations in which the functional space for the unknowns (j, u) is the same as the trial function space. The two formulations differ from the fact that either the velocity or the pressure is sought in a space with more regularity. On the other hand, it is also possible to consider nonsymmetric formulations in which the solution and trial spaces are different. The present work shall focus on one of such formulations, in which both velocity and pressure solution spaces have more regularity than the corresponding trial spaces [12, 13]. Considering for the sake of simplicity homogeneous Dirichlet boundary conditions for the pressure and assuming, as is usual in a posteriori error analysis, that the data f is in $L^2(\Omega)$, the weak formulation of (1.1) may be written as

$$\left\{\begin{array}{ll} \text{Find } (j,u) \in H_{\text{div}}(\Omega) \times H_0^1(\Omega) \text{ such that} & \\ \int_\Omega j \cdot q + \int_\Omega k\, q \cdot \nabla u = 0 & \forall\, q \in (L^2(\Omega))^d\,, \\ \int_\Omega v\, \nabla \cdot j = \int_\Omega f v & \forall\, v \in L^2(\Omega)\,, \end{array}\right. \tag{1.3}$$

where $H_{\text{div}}(\Omega) = \{\, j \in (L^2(\Omega))^d,\ \nabla \cdot j \in L^2(\Omega)\,\}$ and d is the space dimension. Flux boundary conditions may be easily incorporated by considering an appropriate subspace of $H_{\text{div}}(\Omega)$. Elimination of the velocity unknown readily yields the weak formulation of (1.2) in the form

$$\left\{\begin{array}{ll} \text{Find } u \in H_0^1(\Omega) \text{ such that} & \\ \int_\Omega k \nabla u \cdot \nabla v = \int_\Omega f v & \forall\, v \in H_0^1(\Omega)\,. \end{array}\right. \tag{1.4}$$

From a numerical viewpoint, the weak formulation (1.3) is attractive because one may employ a mixed finite element method of Petrov-Galerkin type in which the discrete trial functions are localized at the mesh cells. Therefore, the discrete scheme may be interpreted as a finite volume discretization which *simultaneously* conserves mass and allows for an accurate reconstruction of the velocity field at the cell level. Such schemes are often termed finite volume box schemes. For Darcy equations, the lowest-order finite volume box scheme has been introduced in [12] and further investigated in [13], while higher-order versions have been derived in [14].

The goal of this work is to derive a posteriori estimates yielding upper and lower bounds for the numerical error resulting from nonconforming approximations to (1.3) in a Petrov-Galerkin framework. An upper error bound is important for reliability issues while a lower bound leads to optimal estimates. We shall investigate residual based and hierarchical error indicators. Since the pioneering work of Babuška and Rheinboldt [7], extensive theoretical and computational progress has been achieved in the development of a posteriori error estimates to finite element approximations. For a thorough introduction to residual based a posteriori error estimates of conforming finite element approximations of elliptic equations, we refer to [19]. Early work on a posteriori error estimates derived from the use of hierarchical basis functions includes [8, 9].

Despite important advances achieved in the last few years, a posteriori estimates for "nonstandard" discretization methods, such as finite volume methods and nonconforming finite element methods, are not yet fully developed. On the one hand, recent results on residual based error indicators for Darcy flow simulations are given in [4], where the symmetric formulation of (1.1) relying on a more regular space for the pressure than for the velocity is discretized in both conforming and nonconforming finite element settings. A finite volume interpretation of the degrees of freedom is also given. Additional results on residual based a posteriori estimates for nonconforming approximations of elliptic problems include [17] where the residuals are weighted by coefficients depending on a dual problem, [18] where a post-processing term resulting from the nonconformity of the discrete solution is included in the error indicator and [6] where a general framework for a posteriori estimates to finite element methods with violated Galerkin orthogonality is derived. On the other hand, the extension of hierarchical a posteriori error estimators to a nonconforming setting has been discussed theoretically in [2]. However, applications of this technique to Darcy flows only include the symmetric formulation of the problem with a more regular velocity space discretized by the conforming Raviart-Thomas element [2,20].

This paper is organized as follows. In Section 2, we briefly restate the main results concerning the numerical analysis of the finite volume box scheme considered for the discretization of (1.3). A posteriori error estimates of residual type are investigated in Section 3. Two estimators are derived, one based on the mixed formulation and one based on an equivalent primal formulation for the discrete pressure. A posteriori estimates of hierarchical type are obtained in Section 4. Estimators based on edge bubbles and on element bubbles are investigated. Numerical results are presented in Section 5. Conclusions are drawn in Section 6.

2. Discretization schemes and a priori error analysis

In this section we briefly discuss our basic model assumptions. We then present the discretization schemes for (1.3) and recall the main results concerning their a priori error analysis.

2.1. **Model assumptions and notation**

Let Ω be a bounded polygonal domain in $\mathbb{R}^d$ with $d = 2$ or 3. For the sake of simplicity, we restrict our analysis to isotropic media in which the hydraulic conductivity k is a scalar. However, we shall address the case of heterogeneous media in which the coefficient k undergoes either smooth or sharp variations in the computational domain Ω. Since the hydraulic conductivity results from the geological properties of the porous medium, it is reasonable to make the following assumption [3]:

Hypothesis 2.1. *There exists a partition $\overline{\Omega} = \cup_{l=1}^{L}\overline{\Omega}_l$ with $\Omega_l \cap \Omega_{l'} = \emptyset$ for $l \neq l'$, such that k equals a positive constant k_l in each Ω_l.*

This hypothesis will always be made implicitly in the rest of this work.

For strongly heterogeneous media, the condition ratio of k evaluated as $k_{\max}/k_{\min}$, where $k_{\max}$ and $k_{\min}$ denote respectively the maximum and the minimum value attained by k in Ω, is very large. In this case, it is important from a practical viewpoint that the constants arising in the error estimates be independent of this ratio. To this purpose, it was shown in [10] that an appropriate norm to measure the error in the pressure $u \in H_0^1(\Omega)$ is the energy norm

$$|u|_{k,1} = \left(\sum_{l=1}^{L} k_l \, \|\nabla u\|_{0,\Omega_l}^2\right)^{1/2}. \tag{2.1}$$

For a region R, $\|\cdot\|_{0,R}$ denotes the L^2-norm on R with associated scalar product $(\cdot,\cdot)_{0,R}$ while $|\cdot|_{m,R}$, $m = 1,2$, denotes the Sobolev semi-norm of order m over R. For $\varphi \in L^2(\Omega)$, we shall also make use of the norms $\|\varphi\|_{k^{\pm1},0} = (\sum_{l=1}^{L} k_l^{\pm1}\|\varphi\|_{0,\Omega_l}^2)^{1/2}$. In this work, we are also interested in measuring the error on the velocity since this quantity is essential for accurate contaminant transfer simulation. For $j \in H_{\mathrm{div}}(\Omega)$, we shall consider the norm

$$\|j\|_{k^{-1},\mathrm{div}} = \left(\sum_{l=1}^{L} k_l^{-1} \, \|j\|_{0,\Omega_l}^2 + k_l^{-1} \, \|\nabla \cdot j\|_{0,\Omega_l}^2\right)^{1/2}. \tag{2.2}$$

Let $(\mathcal{T}_h)_h$ be a shape-regular family of triangulations of Ω. For the sake of simplicity, we use the terminology of the $2D$ case, being understood that in the $3D$ case, triangles should be replaced by tetrahedra, edges by faces, etc. In the sequel, we will always make implicitly the following assumption:

Hypothesis 2.2. *For all h, the triangulation $\mathcal{T}_h$ is compatible with the partition $\overline{\Omega} = \cup_{l=1}^{L}\overline{\Omega}_l$ in the sense that the interior of any triangle $T \in \mathcal{T}_h$ has a nonempty intersection with only one of the subdomains Ω_l.*

For a triangle $T \in \mathcal{T}_h$, let h_T be its diameter and set $h = \max_{T\in\mathcal{T}_h} h_T$. Let $\mathcal{E}_h$ and $\mathcal{E}_h^i$ denote respectively the set of edges and internal edges in $\mathcal{T}_h$. For an edge $e \in \mathcal{E}_h$, let h_e be its length, and let $\mathcal{T}_e$ be the set of elements in $\mathcal{T}_h$ containing e. For an element $T \in \mathcal{T}_h$, let $\mathcal{E}_T$ be the set of edges belonging to T. For $e \in \mathcal{E}_h$, choose a unit normal vector n_e. For a piecewise continuous function φ on $\mathcal{T}_h$, $[\varphi]_e$ denotes the jump of φ across e in the direction of n_e, with the convention that a zero outer value is taken for edges contained in $\partial\Omega$.

Because of hypothesis 2.2, the coefficient k is constant on T and its local value will be denoted by k_T. For $e \in \mathcal{E}_h$ such that $e = T \cap T'$ with T and T' in $\mathcal{T}_h$, we set $\overline{k}_e = \frac{1}{2}(k_T + k_{T'})$ and $k_e^+ = \max(k_T, k_{T'})$.

Finally, c shall always denote a positive constant which neither depends on h nor on the ratio $k_{\max}/k_{\min}$.

2.2. The finite volume box scheme

We seek the discrete velocity in the $H_{\text{div}}(\Omega)$-conforming Raviart-Thomas finite element space $RT^0(\mathcal{T}_h)$ of lowest-order and the discrete pressure in the nonconforming Crouzeix-Raviart finite element space

$$P^1_{\text{nc},0}(\mathcal{T}_h) = \{\, v_h \in L^2(\Omega);\ \forall T \in \mathcal{T}_h,\ v_{h|T} \in P^1(T);\ \forall e \in \mathcal{E}_h,\ \int_e [v_h]_e d\sigma = 0 \,\},$$

where $P^1(T)$ is the space of polynomials on T with degree ≤ 1. The trial functions for the pressure and the velocity are both taken in the space of piecewise constant functions $P^0(\mathcal{T}_h)$. The resulting nonconforming mixed finite element discretization of (1.3) corresponds to the finite volume box scheme

$$\left\{\begin{array}{ll} \text{Find } (j_h, u_h) \in RT^0(\mathcal{T}_h) \times P^1_{\text{nc},0}(\mathcal{T}_h) \text{ such that} & \\ \ a(j_h, q_h) + b_h(q_h, u_h) = 0 & \forall\, q_h \in (P^0(\mathcal{T}_h))^d\,, \\ \ b(j_h, v_h) = (f, v_h)_{0,\Omega} & \forall\, v_h \in P^0(\mathcal{T}_h)\,, \end{array}\right. \tag{2.3}$$

with the bilinear forms

$$a(j_h, q_h) = (j_h, q_h)_{0,\Omega}\,, \quad b(j_h, v_h) = (\nabla \cdot j_h, v_h)_{0,\Omega}\,, \quad b_h(q_h, u_h) = \sum_{T\in\mathcal{T}_h} k_T (q_h, \nabla u_h)_{0,T}\,. \tag{2.4}$$

The numerical analysis of scheme (2.3) has been performed in [13] in the case of constant coefficient k. Following similar arguments, it is easily shown that the discrete problem (2.3) is well posed. Furthermore, it is straightforward to verify that the discrete pressure u_h is also the unique solution of the problem

$$\left\{\begin{array}{l} \text{Find } u_h \in P^1_{\text{nc},0}(\mathcal{T}_h) \text{ such that} \\ \displaystyle\sum_{T\in\mathcal{T}_h} k_T (\nabla u_h, \nabla v_h)_{0,T} = (f_h, v_h)_{0,\Omega} \quad \forall v_h \in P^1_{\text{nc},0}(\mathcal{T}_h)\,, \end{array}\right. \tag{2.5}$$

with $f_h = \Pi^0 f$, where Π^0 denotes the orthogonal projector from $L^2(\Omega)$ onto $P^0(\mathcal{T}_h)$. Problem (2.5) will be termed the 'pressure formulation'.

The discrete problem (2.3) satisfies two important properties:

- the discrete velocity j_h may be reconstructed locally from the expression

$$\forall T \in \mathcal{T}_h\,, \quad j_{h|T} = -k_T \nabla u_{h|T} + \frac{1}{2}(f_h \pi_h^1)_{|T}\,, \tag{2.6}$$

  where π_h^1 is a piecewise first-order polynomial such that $\forall T \in \mathcal{T}_h$ and $\forall x = (x_1, \cdots, x_d) \in T$, we have $\pi_h^1(x) = (x_1 - G_{T,1}, \cdots, x_d - G_{T,d})$, $(G_{T,1}, \ldots, G_{T,d})$ being the coordinates of the center of mass of triangle T. For further use, it is convenient to introduce the gyration radius of T given by $\rho_T = \frac{1}{|T|^{1/2}} \|\pi_h^1\|_{0,T}$, where $|T|$ is the measure of T.

- the discrete velocity j_h satisfies the discrete mass conservation equation

$$\nabla \cdot j_h = f_h \,. \tag{2.7}$$

2.3. A priori error analysis

For $v \in H_0^1(\Omega) + P^1_{\mathrm{nc},0}(\mathcal{T}_h)$, we introduce the broken energy norm

$$|v|_{k,h} = \left(\sum_{T\in\mathcal{T}_h} k_T \|\nabla v\|^2_{0,T} \right)^{1/2} \,. \tag{2.8}$$

Proposition 2.3. *Let (j,u) and (j_h,u_h) be respectively the unique solution of (1.1) and (2.3). Then, there exists a constant c such that*

$$\left\{ \begin{array}{l} c|u-u_h|_{k,h} \le h\, \left(\sum_{T\in\mathcal{T}_h} k_T |u|^2_{2,T}\right)^{1/2} + h\|f-f_h\|_{k^{-1},0}\,, \\ \|j-j_h\|_{k^{-1},0} \le \sqrt{2}|u-u_h|_{k,h} + \frac{1}{\sqrt{2}} h\|f_h\|_{k^{-1},0}\,. \end{array}\right. \tag{2.9}$$

Proof. The proof is similar to the one presented in [12] for constant coefficient k and we only highlight the differences arising when k is variable. Since u_h solves the nonconforming finite element problem (2.5), we deduce using classical techniques (see for instance [15]) that

$$|u-u_h|_{k,h} \le 2 \inf_{w_h\in P^1_{\mathrm{nc},0}(\mathcal{T}_h)} |u-w_h|_{k,h} + \sup_{v_h\in P^1_{\mathrm{nc},0}(\mathcal{T}_h)} \frac{(f_h,v_h)_{0,\Omega} - \sum_{T\in\mathcal{T}_h} k_T(\nabla u,\nabla v_h)_{0,T}}{|v_h|_{k,h}} \,.$$

Using standard interpolation techniques locally on each element T, the first term in the r.h.s may be estimated by $c\,h\,\left(\sum_{T\in\mathcal{T}_h} k_T|u|^2_{2,T}\right)^{1/2}$. Concerning the second term, we notice that an integration by parts yields

$$(f_h,v_h)_{0,\Omega} - \sum_{T\in\mathcal{T}_h} k_T(\nabla u,\nabla v_h)_{0,T} = -(f-f_h,v_h)_{0,\Omega} - \sum_{T\in\mathcal{T}_h} k_T \int_{\partial T} \partial_n u\, v_h \,.$$

The first term in the right member is readily estimated as

$$\begin{aligned} (f-f_h,v_h)_{0,\Omega} &= (f-f_h, v_h - \Pi^0 v_h)_{0,\Omega} \\ &\le \|f-f_h\|_{k^{-1},0}\|v_h-\Pi^0 v_h\|_{k,0} \\ &\le c\,h\,\|f-f_h\|_{k^{-1},0}|v_h|_{k,h}\,, \end{aligned} \tag{2.10}$$

whereas classical interpolation techniques (see for instance [11]) yield for the second term

$$\sum_{T\in\mathcal{T}_h} k_T \int_{\partial T} \partial_n u\, v_h \le c\,h \left(\sum_{T\in\mathcal{T}_h} k_T|u|^2_{2,T} \right)^{1/2} |v_h|_{k,h} \,.$$

Combining the above estimates yields the desired upper bound for the pressure error. Finally, the velocity error estimate directly follows from the reconstruction property (2.6) since

$$\begin{aligned} \|j-j_h\|_{k^{-1},0} &\le \left(\sum_{T\in\mathcal{T}_h} 2k_T|u-u_h|^2_{1,T} + \tfrac{1}{2}k_T^{-1}\|f_h\pi_h^1\|^2_{0,T}\right)^{1/2} \\ &\le \sqrt{2}|u-u_h|_{k,h} + \tfrac{1}{\sqrt{2}}h\|f_h\|_{k^{-1},0}\,. \end{aligned}$$

□

Without any additional regularity assumption on the data f, the only estimate available for the divergence of the velocity is

$$\|\nabla \cdot (j - j_h)\|_{k^{-1},0} \leq \|f - f_h\|_{k^{-1},0} \,. \tag{2.11}$$

In most applications, it is reasonable to assume that the data is more regular. Typically, we may assume that the data is H^1 on the subdomains Ω_l,

$$\forall l\,,\ 1 \leq l \leq L\,, \quad f_{|\Omega_l} \in H^1(\Omega_l)\,. \tag{2.12}$$

With this assumption, we readily obtain first-order convergence in the norm $|u - u_h|_{k,h} + \|j - j_h\|_{k^{-1},\mathrm{div}}$, since $h\|f - f_h\|_{k^{-1},0} \leq ch^2 \left(\sum_{T\in\mathcal{T}_h} k_T^{-1} |f|_{1,T}^2\right)^{1/2}$.

3. A posteriori analysis of residual type

In this section we establish two a posteriori error indicators of residual type. The first one is obtained from the mixed formulation (2.3) and the second one from the pressure formulation (2.5). The former presents the drawback that the constants arising in the estimates may depend on the ratio $k_{\max}/k_{\min}$, whereas the latter yields constants independent from this ratio. The numerical experiments presented in section 5 will show that for strongly heterogeneous media, both estimators retain their usefulness.

3.1. Preliminary results

Let $P^1_{\mathrm{c},0}(\mathcal{T}_h) = P^1_{\mathrm{nc},0}(\mathcal{T}_h) \cap H^1_0(\Omega)$ be the conforming finite element space of degree one. In the sequel, we shall often make use of the following hypothesis introduced in [10].

Hypothesis 3.1. *For any two different subdomains $\overline{\Omega}_{l_1}$ and $\overline{\Omega}_{l_2}$ sharing at least one point, there exists a connected path going from $\overline{\Omega}_{l_1}$ to $\overline{\Omega}_{l_2}$ through adjacent subdomains such that the function k is monotone along this path (adjacent means that the corresponding subdomains share an edge).*

Note that in the case of dimension $d = 2$, a sufficient condition for hypothesis 3.1 to hold is that there are at most 3 subdomains sharing a common point in Ω and at most 2 subdomains sharing a common point on $\partial\Omega$.

We consider the two following interpolation operators:

- under hypothesis 3.1, it was proven in [10] that there exists an interpolation operator $\mathcal{I}_{\mathrm{BV}} : H^1_0(\Omega) \to P^1_{\mathrm{c},0}(\mathcal{T}_h)$ such that

$$\forall v \in H^1_0(\Omega), \quad \forall T \in \mathcal{T}_h, \quad \|v - \mathcal{I}_{\mathrm{BV}} v\|_{0,T} \leq c h_T (k_T)^{-1/2} |v|_{k,\Delta_T}\,, \tag{3.1}$$

$$\forall v \in H^1_0(\Omega), \quad \forall e \in \mathcal{E}_h, \quad \|v - \mathcal{I}_{\mathrm{BV}} v\|_{0,e} \leq c h_e^{1/2} (k_e^+)^{-1/2} |v|_{k,\Delta_e}\,, \tag{3.2}$$

  where Δ_T and Δ_e denote respectively the union of all elements $T \in \mathcal{T}_h$ that share at least an edge with T and one vertex with e and where we have used the notation $|v|_{k,\Delta_T} = \|k^{1/2}\nabla v\|_{0,\Delta_T}$ and $|v|_{k,\Delta_e} = \|k^{1/2}\nabla v\|_{0,\Delta_e}$.
- let $\mathcal{I}_{\mathrm{Os}} : P^1_{\mathrm{nc},0}(\mathcal{T}_h) \to P^1_{\mathrm{c},0}(\mathcal{T}_h)$ be the Oswald interpolation operator defined for v_h in $P^1_{\mathrm{nc},0}(\mathcal{T}_h)$ as the unique function in $P^1_{\mathrm{c},0}(\mathcal{T}_h)$ such that for all vertex s in $\mathcal{T}_h$,

$$\mathcal{I}_{\mathrm{Os}} v_h(s) = \frac{1}{\sharp(\mathcal{T}_s)} \sum_{T\in\mathcal{T}_s} v_{h|T}(s)\,,$$

  where $\mathcal{T}_s$ is the set of elements in $\mathcal{T}_h$ containing s and $\sharp(\mathcal{T}_s)$ the cardinal of this set. The Oswald interpolation operator has been considered in [4, 16]. Under hypothesis 3.1, it was proven in [3] that there exists a constant c such that

$$\forall v_h \in P^1_{\mathrm{nc},0}(\mathcal{T}_h), \quad |v_h - \mathcal{I}_{\mathrm{Os}} v_h|_{k,h} \le c \left(\sum_{e \in \mathcal{E}_h^i} \overline{k}_e h_e^{-1} \|[v_h]_e\|^2_{0,e} \right)^{1/2} . \tag{3.3}$$

3.2. Estimator based on the mixed formulation

Proposition 3.2. *Let (j, u) and (j_h, u_h) be respectively the unique solution of (1.3) and (2.3), and let*

$$\mathcal{P}_1(f) = \left(\sum_{T \in \mathcal{T}_h} k_T^{-1} \|f - f_h\|^2_{0,T} + \frac{1}{4} k_T^{-1} \rho_T^2 \|f_h\|^2_{0,T} \right)^{1/2} . \tag{3.4}$$

Then there exists a constant ν independent of h such that

$$|u - u_h|_{k,h} + \|j - j_h\|_{k^{-1},\mathrm{div}} \le \nu \left(\mathcal{P}_1(f) + \inf_{v_h \in P^1_{c,0}(\mathcal{T}_h)} |u_h - v_h|_{k,h} \right) . \tag{3.5}$$

Remark 3.3. The a posteriori error estimate in the right member of (3.5) is the sum of a pre-processing term only depending on the data f and the mesh $\mathcal{T}_h$ plus a post-processing term also depending on the discrete pressure u_h.

Proof. Let v_h be an arbitrary function in $P^1_{\mathrm{nc},0}(\mathcal{T}_h)$ and let $j_h \in RT^0(\mathcal{T}_h)$ be the discrete velocity field. Since (j, u) is the exact solution of problem (1.3), we have

$$\begin{aligned}
a(j_h - j, q) + b_h(q, v_h - u) &= a(j_h, q) + b_h(q, v_h) \\
&= \sum_{T \in \mathcal{T}_h} \int_T (k_T \nabla v_h + j_h) \cdot q \\
&\le \sum_{T \in \mathcal{T}_h} k_T^{1/2} \|\nabla v_h + k_T^{-1} j_h\|_{0,T} \, k_T^{1/2} \|q\|_{0,T} ,
\end{aligned}$$

and

$$\begin{aligned}
b(j_h - j, v) &= b(j_h, v) - (f, v)_{0,\Omega} \\
&= \sum_{T \in \mathcal{T}_h} \int_T (\nabla \cdot j_h - f) \, v \\
&\le \sum_{T \in \mathcal{T}_h} k_T^{-1/2} \|\nabla \cdot j_h - f\|_{0,T} \, k_T^{1/2} \|v\|_{0,T} .
\end{aligned}$$

For $(j, u) \in H_{\mathrm{div}}(\Omega) \times H^1_0(\Omega)$ and $(q, v) \in (L^2(\Omega))^d \times L^2(\Omega)$, consider the bilinear form

$$B((j, u), (q, v)) = a(j, q) + b_h(q, u) + b(j, v) .$$

Since problem (1.3) is well posed, B satisfies an inf-sup condition of the form

$$|u|_{k,h} + \|j\|_{k^{-1},\mathrm{div}} \le \frac{1}{\lambda} \sup_{(q,v) \in (L^2(\Omega))^d \times L^2(\Omega)} \frac{B((j, u), (q, v))}{(\|v\|^2_{k,0} + \|q\|^2_{k,0})^{1/2}} , \tag{3.6}$$

for all $(j,u) \in H_{\mathrm{div}}(\Omega) \times H_0^1(\Omega)$, where λ is a constant independent of h but that may depend on the ratio $k_{\max}/k_{\min}$. This yields

$$|u - v_h|_{k,h} + \|j - j_h\|_{k^{-1},\mathrm{div}} \le \frac{1}{\lambda}\left(\sum_{T\in\mathcal{T}_h} k_T\|k_T^{-1}j_h + \nabla v_h\|_{0,T}^2 + k_T^{-1}\|f - \nabla\cdot j_h\|_{0,T}^2\right)^{1/2}.$$

Since $\nabla \cdot j_h = f_h$ and using the triangle inequality, we obtain

$$|u - v_h|_{k,h} + \|j - j_h\|_{k^{-1},\mathrm{div}} \le \frac{\sqrt{2}}{\lambda}\left(|u_h - v_h|_{k,h}^2 + \|f - f_h\|_{k^{-1},0}^2 + \sum_{T\in\mathcal{T}_h} k_T\|k_T^{-1}j_h + \nabla u_h\|_{0,T}^2\right)^{1/2},$$

and using the reconstruction formula (2.6), we obtain the a posteriori estimate (3.5) with the constant $\nu = \frac{\sqrt{2}}{\lambda}$. □

A possible choice for v_h in (3.5) is the Oswald interpolate of u_h. This yields the following result.

Corollary 3.4. *Let (j,u) and (j_h,u_h) be respectively the unique solution of (1.3) and (2.3). Then, under hypothesis 3.1, there exists a constant ν independent of h such that*

$$|u - u_h|_{k,h} + \|j - j_h\|_{k^{-1},\mathrm{div}} \le \nu\left(\mathcal{P}_1(f) + \eta_1(u_h)\right), \tag{3.7}$$

where

$$\eta_1(u_h) = \left(\sum_{e\in\mathcal{E}_h^i} \overline{k}_e h_e^{-1}\|[u_h]_e\|_{0,e}^2\right)^{1/2}. \tag{3.8}$$

Proof. Follows directly from (3.3). □

Finally, we investigate the optimality of the above error estimators.

Proposition 3.5. *Let (j,u) and (j_h,u_h) be respectively the unique solution of (1.3) and (2.3). Then, there exists a constant c such that*

$$\mathcal{P}_1(f) + \inf_{v_h\in P_{c,0}^1(\mathcal{T}_h)} |u_h - v_h|_{k,h} \le \mathcal{P}_1(f) + \eta_1(u_h) \le c\,|u - u_h|_{k,h} + \sqrt{2}\|j - j_h\|_{k^{-1},\mathrm{div}}. \tag{3.9}$$

Proof. The local reconstruction property (2.6) as well as equations (1.1) and (2.7) yield

$$\begin{aligned}\mathcal{P}_1(f) &= \left(\sum_{T\in\mathcal{T}_h} k_T^{-1}\|\nabla\cdot(j - j_h)\|_{0,T}^2 + k_T^{-1}\|j_h + k_T\nabla u_h\|_{0,T}^2\right)^{1/2}\\ &\le \sqrt{2}\left(\|j - j_h\|_{k^{-1},\mathrm{div}} + |u - u_h|_{k,h}\right).\end{aligned}$$

Furthermore, it was established in [3] that there exists a constant c such that

$$\forall v \in H_0^1(\Omega),\ \forall v_h \in P_{\mathrm{nc},0}^1(\mathcal{T}_h),\ \forall e \in \mathcal{E}_h^i,\quad \overline{k}_e^{1/2} h_e^{-1/2}\|[v_h]\|_{0,e} \le c\sum_{T\in\mathcal{T}_e} k_T^{1/2}|v - v_h|_{1,T}. \tag{3.10}$$

This yields $\eta_1(u_h) \le c|u - u_h|_{k,h}$, which completes the proof. □

3.3. Estimators based on the pressure formulation

In this section we first derive an a posteriori error indicator for the pressure and then deduce an a posteriori error indicator for the velocity.

Proposition 3.6. *Let u and u_h be respectively the unique solution of (1.4) and (2.5). Then, under hypothesis 3.1, there exists a constant c such that*

$$|u-u_h|_{k,h} \leq c\,\mathcal{P}_2(f) + 2 \inf_{v_h\in P^1_{c,0}(\mathcal{T}_h)} |u_h - v_h|_{k,h}\,, \tag{3.11}$$

where

$$\mathcal{P}_2(f) = \left(\sum_{T\in\mathcal{T}_h} 2h_T^2 k_T^{-1}\|f-f_h\|^2_{0,T} + h_T^2 k_T^{-1}\|f_h\|^2_{0,T} + \frac{1}{2}\sum_{e\in\mathcal{E}_T} h_e (k_e^+)^{-1}\|[f_h\pi_h^1\cdot n_e]_e\|^2_{0,e}\right)^{1/2}. \tag{3.12}$$

Proof. For all $w_h \in P^1_{c,0}(\mathcal{T}_h)$, we have

$$\sum_{T\in\mathcal{T}_h} k_T(\nabla(u-u_h),\nabla w_h)_{0,T} = (f-f_h, w_h)_{0,\Omega}\,,$$

and therefore, for all $w\in H^1_0(\Omega)$, we have

$$\sum_{T\in\mathcal{T}_h} k_T(\nabla(u-u_h),\nabla w)_{0,T} = \sum_{T\in\mathcal{T}_h} k_T(\nabla(u-u_h),\nabla(w-w_h))_{0,T} + (f-f_h,w_h)_{0,\Omega}\,.$$

Take $w_h = \mathcal{I}_{\rm BV} w$. Using classical techniques for residual a posteriori estimates [10,19], we obtain

$$\begin{aligned}\sum_{T\in\mathcal{T}_h} k_T(\nabla(u-u_h),\nabla(w-w_h))_{0,T} \quad &\leq\quad c|w|_{k,h}\left(\sum_{T\in\mathcal{T}_h} h_T^2k_T^{-1}\|f_h\|^2_{0,T} + h_T^2k_T^{-1}\|f-f_h\|^2_{0,T}\right.\\ &+\quad \left.\frac{1}{2}\sum_{e\in\mathcal{E}_T} h_e\,(k_e^+)^{-1}\|[k\nabla u_h\cdot n_e]_e\|^2_{0,e}\right)^{1/2}.\end{aligned}$$

From the reconstruction formula (2.6) and the fact that $\forall e\in\mathcal{E}_h$, $[j_h\cdot n_e]_e = 0$ since $j_h\in RT^0(\mathcal{T}_h)$, we deduce that $[k\nabla u_h\cdot n_e]_e = \frac{1}{2}[f_h\pi_h^1\cdot n_e]_e$. Furthermore, the term $(f-f_h,w_h)_{0,\Omega}$ is estimated as in (2.10), yielding

$$\begin{aligned}(f-f_h,w_h)_{0,\Omega} \quad &\leq\quad c\sum_{T\in\mathcal{T}_h} h_T\,k_T^{-1/2}\|f-f_h\|_{0,T}\,k_T^{1/2}\|\nabla w\|_{0,T}\\ &\leq\quad c\left(\sum_{T\in\mathcal{T}_h} h_T^2\,k_T^{-1}\|f-f_h\|^2_{0,T}\right)^{1/2}|w|_{k,h}\,.\end{aligned}$$

Therefore, we have

$$\sum_{T\in\mathcal{T}_h} k_T(\nabla(u-u_h),\nabla w)_{0,T} \leq c\mathcal{P}_2(f)|w|_{k,h}\,.$$

Let v_h be an arbitrary function in $P^1_{c,0}(\mathcal{T}_h)$. Setting $w = u - v_h$, we have

$$|u-v_h|^2_{k,h} = \sum_{T\in\mathcal{T}_h} k_T(\nabla(u-u_h),\nabla w)_{0,T} + k_T(\nabla(u_h-v_h),\nabla w)_{0,T}\,,$$

whence we deduce

$$|u - v_h|_{k,h} \le c\mathcal{P}_2(f) + |u_h - v_h|_{k,h} \,.$$

Finally, the triangle inequality $|u - u_h|_{k,h} \le |u - v_h|_{k,h} + |u_h - v_h|_{k,h}$ yields the desired estimate. □

Corollary 3.7. *Let u and u_h be respectively the unique solution of (1.4) and (2.5). Then, under hypothesis 3.1, there exists a constant c such that*

$$|u - u_h|_{k,h} \le c\Big(\mathcal{P}_2(f) + \eta_1(u_h)\Big) \,. \tag{3.13}$$

Proof. Directly results from (3.11) upon choosing for v_h the Oswald interpolate of u_h. □

We next investigate the optimality of the above error estimators.

Proposition 3.8. *Let u and u_h be respectively the unique solution of (1.4) and (2.5). Then, there exists a constant c such that*

$$\mathcal{P}_2(f) + \inf_{v_h \in P^1_{c,0}(\mathcal{T}_h)} |u_h - v_h|_{k,h} \le \mathcal{P}_2(f) + \eta_1(u_h) \le c\left(|u - u_h|_{k,h} + h\|f - f_h\|_{k^{-1},0}\right) \,. \tag{3.14}$$

Proof. Classical techniques (see for instance [10,19]) show that for all $T \in \mathcal{T}_h$, we have

$$\sum_{T\in\mathcal{T}_h}\sum_{e\in\mathcal{E}_T} (k_e^+)^{-1} h_e \|[k_T \nabla u_h \cdot n_e]_e\|^2_{0,e} \le c\left(|u - u_h|^2_{k,h} + \sum_{T\in\mathcal{T}_h} h_T^2 k_T^{-1}\|f - f_h\|^2_{0,T}\right) ,$$

and

$$\sum_{T\in\mathcal{T}_h} h_T^2 k_T^{-1}\|f_h\|^2_{0,T} \le c\left(|u - u_h|^2_{k,h} + \sum_{T\in\mathcal{T}_h} h_T^2 k_T^{-1}\|f - f_h\|^2_{0,T}\right) .$$

Therefore,

$$c\,\mathcal{P}_2(f) \le |u - u_h|_{k,h} + \left(\sum_{T\in\mathcal{T}_h} h_T^2 k_T^{-1}\|f - f_h\|^2_{0,T}\right)^{1/2} \le |u - u_h|_{k,h} + h\|f - f_h\|_{k^{-1},0} \,,$$

and using estimate (3.10) to control $\eta_1(u_h)$, we obtain the desired result. □

Remark 3.9. If $f \in H^1(\Omega)$, $h\|f - f_h\|_{k^{-1},0}$ is one order higher than $|u - u_h|_{k,h}$ since $h\|f - f_h\|_{k^{-1},0} \le ch^2\|\nabla f\|_{k^{-1},0}$.

One of the attractive features of the finite volume box scheme (2.3) is that velocity error estimates may be readily deduced from pressure error estimates.

Proposition 3.10. *Let (j,u) and (j_h,u_h) be respectively the unique solution of (1.3) and (2.3). Assume that there exists a pressure error indicator $\eta(\mathcal{T}_h, f, u_h)$ depending on the mesh $\mathcal{T}_h$, the data f and the discrete pressure u_h such that*

$$\chi_*\,\eta(\mathcal{T}_h, f, u_h) \le |u - u_h|_{k,h} \le \chi^*\,\eta(\mathcal{T}_h, f, u_h) \,, \tag{3.15}$$

for some constants χ_* and χ^*. Then we have

$$\|j - j_h\|_{k,\mathrm{div}} \le \sqrt{2}\Big(\chi^*\eta(\mathcal{T}_h, f, u_h) + \mathcal{P}_1(f)\Big) \,, \tag{3.16}$$

and

$$\chi_*\eta(\mathcal{T}_h, f, u_h) + \frac{1}{\sqrt{2}}\mathcal{P}_1(f) \le 2|u - u_h|_{k,h} + \sqrt{2}\|j - j_h\|_{k,\mathrm{div}} \,. \tag{3.17}$$

Proof. We first prove estimate (3.16). The local reconstruction property (2.6) yields

$$\|j - j_h\|^2_{k^{-1},0} \le 2 \sum_{T\in\mathcal{T}_h} k_T \|\nabla(u-u_h)\|^2_{0,T} + \frac{1}{4}\rho_T^2 k_T^{-1} \|f_h\|^2_{0,T}\,.$$

Furthermore, we have $\nabla\cdot(j - j_h) = f - f_h$. Therefore, we get

$$\|\nabla\cdot(j-j_h)\|^2_{k^{-1},0} + \|j-j_h\|^2_{k^{-1},0} \le 2\Big((\chi^*)^2\eta(\mathcal{T}_h, f, u_h)^2 + \mathcal{P}_1(f)^2\Big)\,,$$

yielding estimate (3.16). In order to obtain (3.17), we first notice that

$$\mathcal{P}_1(f) \le \|\nabla\cdot(j-j_h)\|_{k^{-1},0} + \left(\sum_{T\in\mathcal{T}_h} \frac{1}{4} k_T^{-1}\rho_T^2 \|f_h\|^2_{0,T}\right)^{1/2}\,,$$

and from the local reconstruction formula (2.6), we deduce

$$\frac{1}{4}\rho_T^2\|f_h\|^2_{0,T} \le 2\Big(\|j-j_h\|^2_{0,T} + k_T^2\|\nabla(u-u_h)\|^2_{0,T}\Big)\,.$$

Therefore,

$$\mathcal{P}_1(f) \le \|\nabla\cdot(j-j_h)\|_{k^{-1},0} + \sqrt{2}\Big(\|j-j_h\|_{k^{-1},0} + |u-u_h|_{k,h}\Big)\,,$$

whence we easily deduce (3.17). □

4. A posteriori analysis of hierarchical type

In this section we derive various hierarchical a posteriori error estimates for the pressure error in the framework of the pressure formulation (2.5). A posteriori error estimates for the velocity may then be easily deduced from proposition 3.10. On the one hand, we shall establish lower and upper bounds for the pressure error using classical techniques based on a saturation property and a strengthened Cauchy-Schwarz inequality [2, 8]. On the other hand, using the technique presented in [1], we shall circumvent the need for these properties.

4.1. **Preliminaries**

Following the framework introduced in [2, 8], the space $P^1_{\mathrm{nc},0}(\mathcal{T}_h)$ shall be enriched as follows

$$\overline{X}_h = P^1_{\mathrm{nc},0}(\mathcal{T}_h) \oplus \widehat{X}_h\,, \tag{4.1}$$

and we shall consider the two following problems:

$$\left\{\begin{array}{l}\text{Find } \overline{u}_h \in \overline{X}_h \text{ such that}\\ \displaystyle\sum_{T\in\mathcal{T}_h} k_T(\nabla\overline{u}_h, \nabla\overline{v}_h)_{0,T} = (f_h, \overline{v}_h)_{0,\Omega} \quad \forall \overline{v}_h \in \overline{X}_h\,,\end{array}\right. \tag{4.2}$$

and

$$\left\{\begin{array}{l}\text{Find } \widehat{u}_h \in \widehat{X}_h \text{ such that}\\ \displaystyle\sum_{T\in\mathcal{T}_h} k_T(\nabla\widehat{u}_h, \nabla\widehat{v}_h)_{0,T} = (f_h, \widehat{v}_h)_{0,\Omega} - \sum_{T\in\mathcal{T}_h} k_T(\nabla u_h, \nabla\widehat{v}_h)_{0,T} \quad \forall \widehat{v}_h \in \widehat{X}_h\,,\end{array}\right. \tag{4.3}$$

where u_h is the unique solution of the pressure problem (2.5). It is clear that problems (4.2) and (4.3) admit a unique solution.

In this work, the space $\widehat{X}_h$ will be constructed using bubble functions. For $T \in \mathcal{T}_h$ with edges e, e', e'', let $\lambda_{e,T}$, $\lambda_{e',T}$, $\lambda_{e'',T}$ be the barycentric coordinates numbered in such a way that λ_e is associated with the vertex opposite to e. We consider the conforming edge bubble $b_e^{\rm c}$ and the nonconforming element bubble $b_T^{\rm nc}$ which may be defined as follows

$$\forall e \in \mathcal{E}_h^i,\ e = T \cap T', \left\{ \begin{array}{lcl} b^{\rm c}_{e|T} & = & d^d \Pi_{e' \neq e} \lambda_{e',T}\,, \\ b^{\rm c}_{e|T'} & = & d^d \Pi_{e' \neq e} \lambda_{e',T'}\,, \\ b^{\rm c}_{e|\Omega \setminus \mathcal{T}_e} & = & 0\,, \end{array} \right.$$

and

$$\forall T \in \mathcal{T}_h, \left\{ \begin{array}{lcl} b^{\rm nc}_{T\,|T} & = & 2 - (d+1) \sum_{e \in \mathcal{E}_T} \lambda_{e,T}^2\,, \\ b^{\rm nc}_{T\,|\Omega \setminus T} & = & 0\,. \end{array} \right.$$

Note that the nonconforming element bubbles are such that

$$\forall T \in \mathcal{T}_h\,,\ \forall e \in \mathcal{E}_h\,, \quad \int_e b_T^{\rm nc} = 0\,. \tag{4.4}$$

Indeed, in 2D, $b_T^{\rm nc}$ vanishes at the two Gauss points with edge barycentric coordinates $(1 \pm \sqrt{1/3})/2$ whereas in 3D, $b_T^{\rm nc}$ vanishes at the three Gauss points with face barycentric coordinates $(2/3, 1/6, 1/6)$. Finally, we introduce the bubble spaces

$$\mathcal{B}_{\rm c}(\mathcal{T}_h) = \mathrm{span}_{e \in \mathcal{E}_h^i} \{b_e^{\rm c}\} \quad \text{and} \quad \mathcal{B}_{\rm nc}(\mathcal{T}_h) = \mathrm{span}_{T \in \mathcal{T}_h} \{b_T^{\rm nc}\}\,.$$

4.2. Hierarchical estimators relying on a saturation property

In this section, we shall make use of the following properties:

Property 4.1 (Saturation property). *There exists a constant $\beta \in (0,1)$ independent of h and of $k_{\max}/k_{\min}$ such that*

$$|u - \overline{u}_h|_{k,h} \leq \beta\, |u - u_h|_{k,h}\,. \tag{4.5}$$

Property 4.2 (Strengthened Cauchy-Schwarz inequality). *There exists a constant $\gamma \in [0,1)$ independent of h and of $k_{\max}/k_{\min}$ such that*

$$\forall v \in P^1_{nc,0}(\mathcal{T}_h),\ \forall w \in \widehat{X}_h, \quad \sum_{T \in \mathcal{T}_h} k_T (\nabla v, \nabla w)_{0,T} \leq \gamma |v|_{k,h} |w|_{k,h}\,. \tag{4.6}$$

Two hierarchical error estimates are derived in this section, one based on edge bubbles and one based on element bubbles.

4.2.1. *Involving edge bubbles*

In this section we choose $\widehat{X}_h = \mathcal{B}_{\rm c}(\mathcal{T}_h)$.

Proposition 4.3. *Let u and u_h be respectively the unique solution of (1.4) and (2.5). Then, under the saturation property 4.1 and the strengthened Cauchy-Schwarz inequality 4.2, there exists a constant c such that*

$$|u - u_h|_{k,h} \leq c\, \eta_2(u_h)\,, \tag{4.7}$$

where

$$\eta_2(u_h) = |\widehat{u}_h|_{k,h}\,. \tag{4.8}$$

Proof. The proof extends to the nonconforming case the ideas presented in [8]. For $\overline{u}_h \in \overline{X}_h$, we have the unique decomposition $\overline{u}_h = u_1 + u_2$ where $u_1 \in P^1_{\mathrm{nc},0}(\mathcal{T}_h)$ and $u_2 \in \mathcal{B}_{\mathrm{c}}(\mathcal{T}_h)$. For $v_h \in P^1_{\mathrm{nc},0}(\mathcal{T}_h) \subset \overline{X}_h$, we have

$$\sum_{T\in\mathcal{T}_h} k_T(\nabla(\overline{u}_h - u_h), \nabla v_h)_{0,T} = 0\,,$$

and for all $\widehat{v}_h \in \mathcal{B}_{\mathrm{c}}(\mathcal{T}_h)$, we have

$$\sum_{T\in\mathcal{T}_h} k_T(\nabla(\overline{u}_h - u_h), \nabla \widehat{v}_h)_{0,T} = \sum_{T\in\mathcal{T}_h} k_T(\nabla \widehat{u}_h, \nabla \widehat{v}_h)_{0,T}\,.$$

Thus, by taking $v_h = u_1 - u_h$ and $\widehat{v}_h = u_2$ in the above equations, we obtain

$$|\overline{u}_h - u_h|^2_{k,h} = \sum_{T\in\mathcal{T}_h} k_T(\nabla \widehat{u}_h, \nabla u_2)_{0,T}\,,$$

and from the (standard) Cauchy-Schwarz inequality, we deduce $|\overline{u}_h - u_h|^2_{k,h} \le |\widehat{u}_h|_{k,h}|u_2|_{k,h}$. Furthermore, using the strengthened Cauchy-Schwarz property 4.2 yields

$$|u_1 - u_h|^2_{k,h} + |u_2|^2_{k,h} - |\overline{u}_h - u_h|^2_{k,h} = 2\sum_{T\in\mathcal{T}_h} k_T(\nabla u_2, \nabla(u_h - u_1))_{0,\Omega} \le 2\gamma|u_2|_{k,h}|u_h - u_1|_{k,h}\,.$$

Therefore, we obtain $(1-\gamma^2)|u_2|^2_{k,h} \le |\overline{u}_h - u_h|^2_{k,h}$ and combining the above inequalities leads to

$$|u - u_h|_{k,h} \le |u - \overline{u}_h|_{k,h} + \frac{1}{\sqrt{1-\gamma^2}}|\widehat{u}_h|_{k,h}\,.$$

Finally, using the saturation property (4.5), we obtain

$$|u - u_h|_{k,h} \le \frac{1}{(1-\beta)\sqrt{1-\gamma^2}}|\widehat{u}_h|_{k,h}\,, \tag{4.9}$$

yielding the desired result. □

In the two-dimensional case, it is relatively straightforward to verify the strengthened Cauchy-Schwarz property.

Lemma 4.4. *Assume $d = 2$. Then, there exists a constant $\gamma < 1$ only depending on the minimum angle of the triangles in $\mathcal{T}_h$ such that (4.6) is verified.*

Proof. (i) For $T \in \mathcal{T}_h$, let $\mathcal{B}_c(T) = \mathrm{span}_{e\in T}\{b^{\mathrm{c}}_{e|T}\}$ and let

$$\gamma_T = \max_{u\in P^1(T), v\in\mathcal{B}_c(T)} \frac{(\nabla u, \nabla v)_{0,T}}{\|\nabla u\|_{0,T}\|\nabla v\|_{0,T}}\,.$$

In [5], it is shown that $\gamma_T = \sup_{x\in\mathbb{R}^3} \frac{x^t A_{12}A_{22}^{-1}A_{21}x}{x^t A_{11} x}$, where A_{11}, A_{12}, A_{21}, A_{22} are such that the local stiffness matrix A, relative to the basis functions of $P^1_{\mathrm{nc},0}(\mathcal{T}_h)$ and $\mathcal{B}_{\mathrm{c}}(\mathcal{T}_h)$, is $A = \begin{pmatrix} A_{11} & A_{12} \\ A_{21} & A_{22} \end{pmatrix}$.
(ii) We next verify numerically that there exists a constant $\gamma_0 < 1$ only depending on the minimum angle of T such that $\gamma_T \le \gamma_0$. Because of isotropy and scale invariance, we can assume that two of the vertices of triangle T have coordinates $(0,0)$ and $(1,0)$ and parameterize the triangle T by its angles (α,β) (see left plot

in figure 1). For each (α, β), we may solve the above eigenvalue problem numerically and thus construct the function $(\alpha, \beta) \mapsto \gamma_T$. Again, because of isotropy and scale invariance, the same result is obtained for γ_T if any two angles are taken from the set $\{\alpha, \beta, \pi - \alpha - \beta\}$ in whichever order. Therefore, we may restrict our investigation to the domain

$$D = \{(\alpha, \beta);\ \alpha \geq \beta;\ \alpha + 2\beta \geq \pi;\ \alpha + \beta \leq \pi\}.$$

This domain is depicted in the middle plot of figure 1 as a shaded triangle. Isocontours for the function $(\alpha, \beta) \in D \mapsto \gamma_T$ are presented on the right plot in figure 1. The minimum value for γ_T is 0.5 and is attained for an equilateral triangle (left corner of shaded triangle). Furthermore, we have $\gamma_T \leq 1$ for all (α, β) and $\gamma_T \to 1$ only if $(\alpha, \beta) \to (\pi, 0)$. Since the family of triangulations $(\mathcal{T}_h)_h$ is assumed to be shape-regular, the minimum angle of T may be uniformly bounded from below by a positive quantity. Therefore, it is possible to bound γ_T from above by a constant $\gamma_0 < 1$ only depending on this minimum angle.
(iii) In order to prove (4.6), consider $v_h \in P^1_{\mathrm{nc},0}(\mathcal{T}_h)$ and $w_h \in \mathcal{B}_{\mathrm{c}}(\mathcal{T}_h)$. From the above result, we deduce that

$$\sum_{T \in \mathcal{T}_h} k_T (\nabla v_h, \nabla w_h)_{0,T} \leq \sum_{T \in \mathcal{T}_h} k_T \gamma_T \|\nabla v_h\|_{0,T} \|\nabla w_h\|_{0,T}\,,$$

and using the Cauchy-Schwarz inequality, we obtain

$$\sum_{T \in \mathcal{T}_h} k_T (\nabla v_h, \nabla w_h)_{0,T} \leq \left(\sup_{T \in \mathcal{T}_h} \gamma_T\right) |v_h|_{k,h} |w_h|_{k,h}\,,$$

whence we deduce property 4.2 with the constant $\gamma = \sup_{T \in \mathcal{T}_h} \gamma_T \leq \gamma_0 < 1$. □

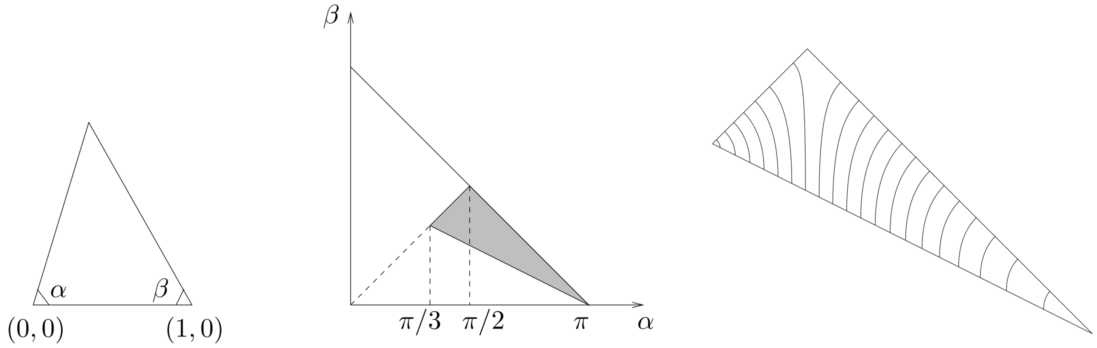

FIGURE 1. Left: triangle T with angles α and β; middle: domain D (shaded triangle) for pairs (α, β); right: isocontours of the function $(\alpha, \beta) \in D \mapsto \gamma_T$

Finally, we investigate the optimality of the above error estimators.

Proposition 4.5. *Let u and u_h be respectively the unique solution of (1.4) and (2.5). Then, there exists a constant c such that*

$$\eta_2(u_h) \leq |u - u_h|_{k,h} + c\,h\|f - f_h\|_{k^{-1},0}\,. \tag{4.10}$$

Proof. Since $\widehat{u}_h$ is the solution of (4.3) and $\widehat{X}_h$ is $H^1_0(\Omega)$-conforming space, we have

$$
\begin{aligned}
|\widehat{u}_h|^2_{k,h} &= \sum_{T\in\mathcal{T}_h}\int_T k_T\nabla(u-u_h)\cdot\nabla\widehat{u}_h + \int_\Omega (f_h-f)\,\widehat{u}_h \\
&= \sum_{T\in\mathcal{T}_h}\int_T k_T\nabla(u-u_h)\cdot\nabla\widehat{u}_h + \int_\Omega (f_h-f)\,(\widehat{u}_h-\Pi^0\widehat{u}_h) \\
&\le |u-u_h|_{k,h}|\widehat{u}_h|_{k,h} + c\,h\|f-f_h\|_{k^{-1},0}\,|\widehat{u}_h|_{k,h}\,,
\end{aligned}
$$

yielding the desired estimate. □

Remark 4.6. In dimension $d=2$, a straightforward calculation shows that

$$
\overline{X}_h = \left\{ v_h\in L^2(\Omega);\ \forall T\in\mathcal{T}_h,\ v_{h|T}\in P^2(T);\ \forall e\in\mathcal{E}_h\ \int_e [v_h]_e = 0 \text{ and } [v_h]_e(m_e)=0 \right\}\,,
$$

where m_e is the midpoint of edge e.

4.2.2. *Involving element bubbles*

In this section we choose $\widehat{X}_h = \mathcal{B}_{\mathrm{nc}}(\mathcal{T}_h)$.

Lemma 4.7. *(i) The strengthened Cauchy-Schwarz constant for spaces $P^1_{nc,0}(\mathcal{T}_h)$ and $\mathcal{B}_{nc}(\mathcal{T}_h)$ is identically 0. (ii) Let $\overline{u}_h = u_1+u_2$ be the unique decomposition of the solution $\overline{u}_h$ of (4.2) with $u_1\in P^1_{nc,0}(\mathcal{T}_h)$ and $u_2\in\mathcal{B}_{nc}(\mathcal{T}_h)$. Then $u_1=u_h$ is the unique solution of (2.5) and $u_2=\widehat{u}_h$ is the unique solution of (4.3).*

Proof. (i) Let v_b be an arbitrary function in $\mathcal{B}_{\mathrm{nc}}(\mathcal{T}_h)$ and v_h an arbitrary function in $P^1_{\mathrm{nc},0}(\mathcal{T}_h)$. The Green formula yields

$$
k_T(\nabla v_b,\nabla v_h)_{0,T} = k_T\sum_{e\in\partial T}\nabla v_h\cdot n_e\int_e v_b\,,
$$

and the right member vanishes thanks to (4.4). This implies that the strengthened Cauchy-Schwarz constant for $P^1_{\mathrm{nc},0}(\mathcal{T}_h)$ and $\mathcal{B}_{\mathrm{nc}}(\mathcal{T}_h)$ is simply 0.
(ii) For all $v_h\in P^1_{\mathrm{nc},0}(\mathcal{T}_h)$, we have

$$
(f_h,v_h)_{0,\Omega} = \sum_{T\in\mathcal{T}_h} k_T(\nabla\overline{u}_h,\nabla v_h)_{0,T} = \sum_{T\in\mathcal{T}_h} k_T(\nabla u_1,\nabla v_h)_{0,T} + \sum_{T\in\mathcal{T}_h} k_T(\nabla u_b,\nabla v_h)_{0,T}\,,
$$

and by using the first part of the proof, we deduce that

$$
\sum_{T\in\mathcal{T}_h} k_T(\nabla u_1,\nabla v_h)_{0,T} = \sum_{T\in\mathcal{T}_h}(f_h,v_h)_{0,T}\quad \forall v_h\in P^1_{\mathrm{nc},0}(\mathcal{T}_h)\,.
$$

Therefore, u_1 is the unique solution of (2.5) and this in turn implies that u_2 is the unique solution of (4.3). □

Proposition 4.8. *Let u and u_h be respectively the unique solution of (1.4) and (2.5). Then, under the saturation property (4.5), we have*

$$
\frac{1}{1+\beta}\mathcal{P}_3(f) \le |u-u_h|_{k,h} \le \frac{1}{1-\beta}\mathcal{P}_3(f)\,, \tag{4.11}
$$

where

$$
\mathcal{P}_3(f) = \left(\sum_{T\in\mathcal{T}_h}\frac{k_T^{-1}(f_h,b_T^{\mathrm{nc}})^2_{0,T}}{|b_T^{\mathrm{nc}}|^2_{1,T}}\right)^{1/2}. \tag{4.12}
$$

Proof. Let $\overline{u}_h$ be the unique solution of (4.2). From lemma 4.7, we have the decomposition $\overline{u}_h = u_h + \widehat{u}_h$. Therefore, we have

$$|\widehat{u}_h|_{k,h} = |\overline{u}_h - u_h|_{k,h} \leq |u - \overline{u}_h|_{k,h} + |u - u_h|_{k,h} \leq (1+\beta)|u - u_h|_{k,h}\,,$$

thanks to the saturation property 4.1. Furthermore, since the constant γ for the strengthened Cauchy-Schwarz inequality is simply 0, we deduce from (4.9) that $|u - u_h|_{k,h} \leq \frac{1}{1-\beta}|\widehat{u}_h|_{k,h}$. As a result, we get

$$\frac{1}{1+\beta}|\widehat{u}_h|_{k,h} \leq |u - u_h|_{k,h} \leq \frac{1}{1-\beta}|\widehat{u}_h|_{k,h}\,,$$

and in order to conclude the proof, we only need to show that $|\widehat{u}_h|_{k,h} = \mathcal{P}_3(f)$. Taking $\widehat{v}_h = b_T^{\mathrm{nc}}$ in (4.3) and using the fact that $\sum_{T\in\mathcal{T}_h} k_T(u_h, b_T^{\mathrm{nc}})_{0,T} = 0$, we get

$$k_T(\nabla\widehat{u}_h, \nabla b_T^{\mathrm{nc}})_{0,T} = (f_h, b_T^{\mathrm{nc}})_{0,T}\,.$$

Let $\widehat{u}_{h|T} = \alpha_T b_T^{\mathrm{nc}}$ for some $\alpha_T \in \mathbb{R}$. Since $(\nabla\widehat{u}_h, \nabla b_T^{\mathrm{nc}})_{0,T} = \alpha_T |b_T^{\mathrm{nc}}|^2_{1,T}$, we obtain

$$\alpha_T = \frac{(f_h, b_T^{\mathrm{nc}})_{0,T}}{k_T|b_T^{\mathrm{nc}}|^2_{1,T}}\,,$$

showing that $|\widehat{u}_h|_{k,h} = \mathcal{P}_3(f)$. □

Remark 4.9. Since $\overline{u}_h$ can be computed without solving problem (4.2), it is straightforward to verify the saturation property numerically.

Remark 4.10. The a posteriori error estimate (4.11) only involves a pre-processing term.

4.3. Hierarchical estimator circumventing the saturation property

In this section we establish a hierarchical a posteriori error estimator that neither requests property 4.1 nor property 4.2. We consider the case $\overline{X}_h = \mathcal{B}_{\mathrm{c}}(\mathcal{T}_h)$.

Proposition 4.11. *Let u and u_h be respectively the unique solution of (1.4) and (2.5). Then, under hypothesis 3.1, there exists a constant c such that*

$$|u - u_h|_{k,h} \leq c\left(\mathcal{P}_4(f) + |\widehat{u}_h|_{k,h} + \inf_{v_h\in P^1_{c,0}(\mathcal{T}_h)} |u_h - v_h|_{k,h}\right), \tag{4.13}$$

where

$$\mathcal{P}_4(f) = \left(\sum_{T\in\mathcal{T}_h} h_T^2\,k_T^{-1}\|f - f_h\|^2_{0,T} + h_T^2\,k_T^{-1}\|f\|^2_{0,T} + h_T^2\underline{k}_T^{-1}\|f_h\|^2_{0,T}\right)^{1/2}, \tag{4.14}$$

and $\underline{k}_T^{-1} = \sum_{e\in\mathcal{E}_T}(k_e^+)^{-1}$.

Proof. Let $\Pi : H^1_0(\Omega) \to \mathcal{B}_{\mathrm{c}}(\mathcal{T}_h)$ be the interpolation operator defined for $v \in H^1_0(\Omega)$ as

$$\Pi v = \sum_{e\in\mathcal{E}_T}\left(\frac{\int_e v}{\int_e b_e^{\mathrm{c}}}\right) b_e^{\mathrm{c}}\,.$$

For all $v_h \in P^1(T)$ and $v \in H_0^1(\Omega)$, an integration by parts readily shows that $\int_T \nabla v_h \cdot \nabla(v - \Pi v) = 0$. Furthermore, for $w \in H_0^1(\Omega)$, we have

$$\begin{aligned}\sum_{T\in\mathcal{T}_h} k_T(\nabla(u-u_h),\nabla w)_{0,T} &= \sum_{T\in\mathcal{T}_h} k_T(\nabla u, \nabla(w-\mathcal{I}_{\mathrm{BV}}w))_{0,T} + k_T(\nabla u, \nabla\mathcal{I}_{\mathrm{BV}}w)_{0,T} \\ &\quad - k_T(\nabla u_h, \nabla(w-\mathcal{I}_{\mathrm{BV}}w))_{0,T} - k_T(\nabla u_h, \nabla\mathcal{I}_{\mathrm{BV}}w)_{0,T} \\ &= \sum_T (f, w-\mathcal{I}_{\mathrm{BV}}w)_{0,T} - k_T(\nabla u_h, \nabla\Pi(w-\mathcal{I}_{\mathrm{BV}}w))_{0,T} \\ &\quad + (f-f_h, \mathcal{I}_{\mathrm{BV}}w)_{0,T}\,.\end{aligned}$$

Since $\widehat{u}_h$ is the solution of problem (4.3) and $\Pi(w - \mathcal{I}_{\mathrm{BV}}w) \in \mathcal{B}_{\mathrm{c}}(\mathcal{T}_h)$, we have

$$\begin{aligned}\sum_{T\in\mathcal{T}_h} k_T(\nabla(u-u_h),\nabla w)_{0,T} &= \sum_{T\in\mathcal{T}_h} (f, w-\mathcal{I}_{\mathrm{BV}}w)_{0,T} - (f_h, \Pi(w-\mathcal{I}_{\mathrm{BV}}w))_{0,T} \\ &+ \quad k_T(\nabla\widehat{u}_h, \nabla\Pi(w-\mathcal{I}_{\mathrm{BV}}w))_{0,T} + (f-f_h, \mathcal{I}_{\mathrm{BV}}w)_{0,T}\,.\end{aligned}$$

Furthermore, it is shown in [1] that the operator Π verifies the following property: there exists a constant c such that for all $v \in H_0^1(\Omega)$, $\|\Pi v\|_{1,T} \le c\, h_T^{-1/2} \sum_{e\in\mathcal{E}_T} \|v\|_{0,e}$. Therefore, we deduce from (3.2) that

$$\begin{aligned}k_T(\nabla\widehat{u}_h, \nabla\Pi(w-\mathcal{I}_{\mathrm{BV}}w))_{0,T} &\le c k_T \|\nabla\widehat{u}_h\|_{0,T} h_T^{-1/2} \sum_{e\in\mathcal{E}_T} \|w-\mathcal{I}_{\mathrm{BV}}w\|_{0,e} \\ &\le c k_T \|\nabla\widehat{u}_h\|_{0,T} h_T^{-1/2} \sum_{e\in\mathcal{E}_T} h_e^{1/2}(k_e^+)^{-1/2} |w|_{k,\Delta_e} \\ &\le c k_T^{1/2} \|\nabla\widehat{u}_h\|_{0,T} \sum_{e\in\mathcal{E}_T} |w|_{k,\Delta_e}\,.\end{aligned}$$

Furthermore, since the family $(\mathcal{T}_h)_h$ is shape-regular, there exists a constant c such that for all $v \in H_0^1(\Omega)$, $\|\Pi v\|_{0,T} \le c h_T^{1/2} \|\Pi v\|_{1,T}$. Therefore, we may write

$$\begin{aligned}(f_h, \Pi(w-\mathcal{I}_{\mathrm{BV}}w))_{0,T} &\le c\|f_h\|_{0,T} h_T^{1/2} \sum_{e\in\mathcal{E}_T} \|w-\mathcal{I}_{\mathrm{BV}}w\|_{0,e} \\ &\le c h_T \|f_h\|_{0,T} \sum_{e\in\mathcal{E}_T} (k_e^+)^{-1/2} |w|_{k,\Delta_e} \\ &\le c k_T^{-1/2} h_T \|f_h\|_{0,T} \sum_{e\in\mathcal{E}_T} |w|_{k,\Delta_e}\,.\end{aligned}$$

Similarly, we may write

$$(f, w-\mathcal{I}_{\mathrm{BV}}w)_{0,T} \le c k_T^{-1/2} h_T \|f\|_{0,T} \sum_{e\in\mathcal{E}_T} |w|_{k,\Delta_e}\,,$$

and

$$(f-f_h, \mathcal{I}_{\mathrm{BV}}w)_{0,T} \le c k_T^{-1/2} h_T \|f-f_h\|_{0,T} \sum_{e\in\mathcal{E}_T} |w|_{k,\Delta_e}\,.$$

Therefore, we get

$$\sum_{T\in\mathcal{T}_h} k_T(\nabla(u-u_h),\nabla w)_{0,T} \le c\left(\mathcal{P}_4(f) + |\widehat{u}_h|_{k,h}\right)|w|_{k,h}\,.$$

Let $v_h \in P^1_{\mathrm{nc},0}(\mathcal{T}_h)$ and let $w = u - v_h$. From the identity

$$|w|^2_{k,h} = \sum_{T\in\mathcal{T}_h} k_T(\nabla(u-u_h),\nabla w)_{0,T} + k_T(\nabla(u_h - v_h),\nabla w)_{0,T}\,,$$

we readily deduce the desired etimate. □

A possible choice for v_h in (4.13) is the Oswald interpolate of u_h. This yields the following result.

Corollary 4.12. *Let u and u_h be respectively the unique solution of (1.4) and (2.5). Then, under hypothesis 3.1, there exists a constant c such that*

$$|u-u_h|_{k,h} \le c\left(\mathcal{P}_4(f) + \eta_3(u_h)\right), \tag{4.15}$$

with

$$\eta_3(u_h) = |\widehat{u}_h|_{k,h} + \eta_1(u_h)\,. \tag{4.16}$$

Proof. Follows directly from (3.3). □

Finally, we investigate the optimality of the above error estimators.

Proposition 4.13. *Let u and u_h be respectively the unique solution of (1.4) and (2.5). Then, there exists a constant c such that*

$$\mathcal{P}_4(f) + \inf_{v_h\in P^1_{c,0}(\mathcal{T}_h)} |u_h - v_h|_{k,h} \le \mathcal{P}_4(f) + \eta_1(u_h) \le c\left(|u-u_h|_{k,h} + h\|f-f_h\|_{k^{-1},0}\right)\,. \tag{4.17}$$

Proof. Classical techniques [10,19] show that for all $T\in\mathcal{T}_h$, we have

$$\begin{aligned}\sum_{T\in\mathcal{T}_h} h_T^2\underline{k}_T^{-1}\|f_h\|^2_{0,T} + h_T^2 k_T^{-1}\|f\|^2_{0,T} &\le c\sum_{T\in\mathcal{T}_h} h_T^2\underline{k}_T^{-1}\|f_h\|_{0,T} + h_T^2 k_T^{-1}\left(\|f-f_h\|^2_{0,T} + \|f_h\|^2_{0,T}\right)\\ &\le c\left(|u-u_h|^2_{k,h} + \sum_{T\in\mathcal{T}_h} h_T^2 k_T^{-1}\|f-f_h\|^2_{0,T}\right),\end{aligned}$$

yielding

$$\mathcal{P}_4(f) \le c\left(|u-u_h|_{k,h} + h\|f-f_h\|_{k^{-1},0}\right)\,.$$

Using estimate (3.10) to control $\eta_1(u_h)$, we obtain the desired result. □

5. Numerical results

In this section we discuss our numerical results. We first consider the case of constant conductivity and then assess our estimators in the case of heterogeneous media.

5.1. Constant conductivity

As a test problem, we consider the unit 2D square $\Omega =]0,1[^2$ with homogeneous Dirichlet boundary conditions and constant conductivity $k=1$. The data f is chosen so that the exact solution of (1.4) is $u(x,y) = \sin(2\pi x)\sin(2\pi y)$. Two families of unstructured triangulations are considered. The first one is a quasi-uniform triangulation with triangle size $h_i = h_0 2^{-i}$, $h_0 = 0.2$ and $i = 0,1,2,3,4$. The second one is strongly non-uniform with triangle size near the boundary as before and triangles ten times smaller in the vicinity of the point $(0.5, 0.5)$ located at the center of Ω. In the figures below, error indicators and numerical errors will be plotted as a function of the number of degrees of freedom for the discrete pressure problem, i.e.

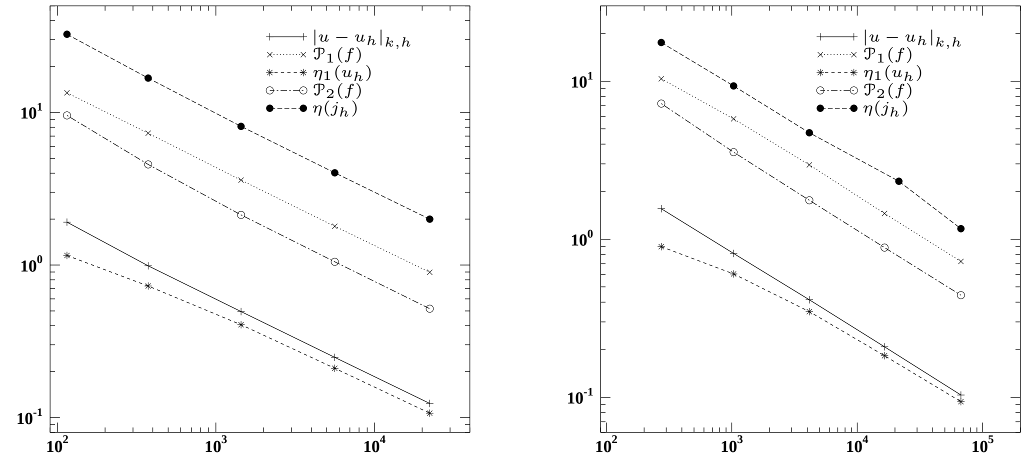

FIGURE 2. Exact error and residual based error indicators as a function of the number of edges in the mesh; left: quasi-uniform triangulation, right: strongly non-uniform triangulation

the number of edges in the mesh. With a log-log scale, first-order convergence therefore yields slopes of 1/2 for two-dimensional problems.

Figure 2 presents our numerical results for the residual based error indicators derived in Section 3 and for the two families of meshes. We present the exact pressure error $|u-u_h|_{k,h}$, the pre-processing term $\mathcal{P}_1(f)$ given by (3.4), the post-processing term $\eta_1(u_h)$ given by (3.8), the pre-processing term $\mathcal{P}_2(f)$ given by (3.12) and the velocity error indicator

$$\eta(j_h) = \eta_1(u_h) + \mathcal{P}_1(f) + \mathcal{P}_2(f)\,,$$

resulting from Corollary 3.7 and Proposition 3.10 by setting the constants equal to one. We first observe that the exact pressure error is first-order in the mesh size, in agreement with the a priori error analysis. All the a posteriori error indicators also exhibit the correct order of convergence. We also notice that the pre-processing term $\mathcal{P}_1(f)$ dominates the post-processing term $\eta_1(u_h)$. As a result, the exact velocity error $\|j-j_h\|_{k^{-1},\mathrm{div}}$ approximately coincides with the pre-processing term $\mathcal{P}_1(f)$. The effectivity index for the pressure error indicator $\eta_1(u_h)$, defined as

$$I_1 = \frac{\eta_1(u_h)}{|u-u_h|_{k,h}}\,,$$

takes values ranging from 0.60 to 0.86. The effectivity index for the total error indicator based on the mixed formulation, defined as

$$I_2 = \frac{\eta_1(u_h) + \mathcal{P}_1(f)}{|u-u_h|_{k,h} + \|j-j_h\|_{k^{-1},\mathrm{div}}}\,,$$

takes values ranging from 0.85 to 0.87. Finally, the effectivity index for the velocity error indicator based on the pressure formulation, defined as

$$I_3 = \frac{\eta_1(u_h) + \mathcal{P}_1(f) + \mathcal{P}_2(f)}{\|j-j_h\|_{k^{-1},\mathrm{div}}}\,,$$

takes values ranging from 1.7 to 1.8. These slightly larger values are due to the presence of the pre-processing term $\mathcal{P}_2(f)$. Thus, we conclude that although the a posteriori estimate based on the pressure formulation is interesting for theoretical reasons since it yields constants independent of the ratio $k_{\max}/k_{\min}$, it presents the numerical drawback to be less sharp than the estimators based on the mixed formulation.

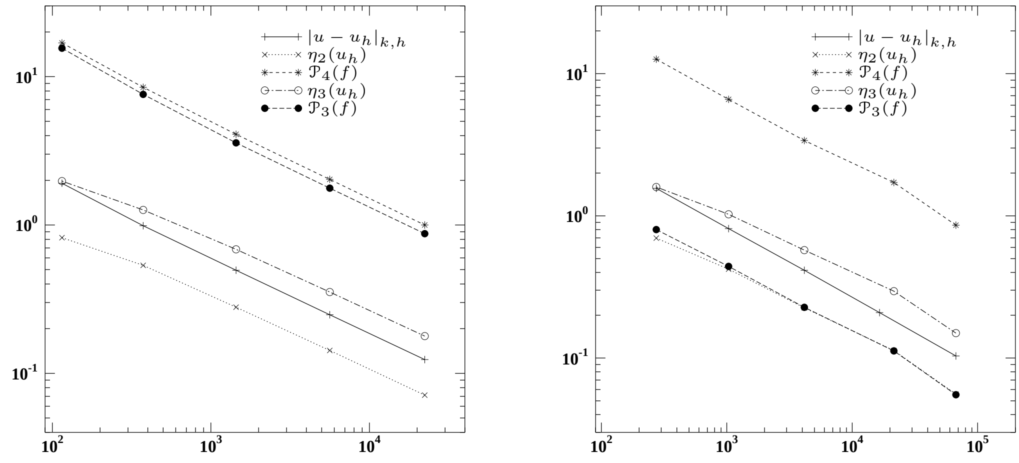

FIGURE 3. Hierarchical error indicators as a function of the number of edges in the mesh; left: quasi-uniform triangulation, right: strongly non-uniform triangulation

Figure 3 displays our numerical results for the hierarchical error indicators derived in Section 4 and for the two families of meshes. We consider the error indicator $\eta_2(u_h)$ given by (4.8) (based on edge bubbles and a saturation property), the pre-processing error estimator $\mathcal{P}_3(f)$ given by (4.12) (based on element bubbles) and the pre-processing and post-processing error indicators $\mathcal{P}_4(f)$ and $\eta_3(u_h)$ given by (4.14) and (4.16) (based on edge bubbles plus a post-processing term). In all cases, the correct order of convergence is obtained. For nonconforming element bubbles, the saturation property has been verified numerically. The constant β was found to be equal to 0.82 for the quasi-uniform meshes and to 0.84 for the non-uniform meshes, thereby confirming that the saturation property is indeed satisfied in this case. Although the saturation property cannot be guaranteed theoretically for conforming edge bubbles, we notice that the estimator $\eta_2(u_h)$ performs well numerically for both quasi-uniform and non-uniform meshes. For the two estimators relying on the saturation property, the effectivity indices for the pressure error indicator, defined as

$$I_4 = \frac{\eta_3(u_h)}{|u-u_h|_{k,h}} \qquad \text{and} \qquad I_5 = \frac{\mathcal{P}_3(f)}{|u-u_h|_{k,h}},$$

are in the range $0.4 - 0.5$ independently of h. The estimator $\mathcal{P}_4(f) + \eta_3(u_h)$ has the theoretical advantage of circumventing the saturation property, but at the expense of numerical effectiveness since the effectivity index is approximately 10.

5.2. **Variable conductivity**

As a test problem, we consider the square $\Omega =]-1,1[^2$ with homogeneous Dirichlet boundary conditions. The domain Ω is split into $L = 4$ four square sub-domains Ω_l with sides of length 1. Subdomains are numbered counter-clockwise starting with the upper right one. On each subdomain Ω_l, the conductivity is set to $k_l = \kappa^{l-1}$. We consider two cases for parameter κ: a mildly varying case where $\kappa = 1.2$ and a strongly heterogeneous one where $\kappa = 10$. Note that the variations of coefficient k are compatible with hypothesis 3.1. In both cases, the data f is $f(x,y) = 2\pi^2 \sin(\pi x)\sin(\pi y)$ so that the exact solution is given by $u(x,y) = \frac{1}{\kappa}\sin(\pi x)\sin(\pi y)$.

Numerical results are presented on a family of quasi-uniform, unstructured triangulations with triangle size $h_i = h_0 2^{-i}$, $h_0 = 0.2$ and $i = 0,1,2,3,4$. Note that the triangulations are always compatible with the sub-domains Ω_l, in agreement with hypothesis 2.2. Figure 4 presents the exact pressure error as well as the same residual based error estimators as those considered in figure 2. The left plot in figure 4 deals with the mildly varying case. We observe that the correct order of convergence is obtained. The right plot of this figure is concerned with the strongly varying case. No degradation in the effectivity indices is observed, confirming that the various error estimators are independent of the ratio $k_{\max}/k_{\min}$. In particular, we notice that the residual error estimator based on the mixed formulation remains well behaved even if the ratio $k_{\max}/k_{\min}$ is very large. Furthermore, the only relevant difference between the mildly and strongly varying cases concerns the error indicator $\eta_1(u_h)$ which for the coarsest meshes and strongly varying coefficient exhibits super-convergence behavior but takes larger values than those observed in the mildly varying case. This phenomenon is due to the fact that the pressure jumps are maximal at the sub-domain interfaces where the edge-averaged conductivity $\overline{k}_e$ may be very large.

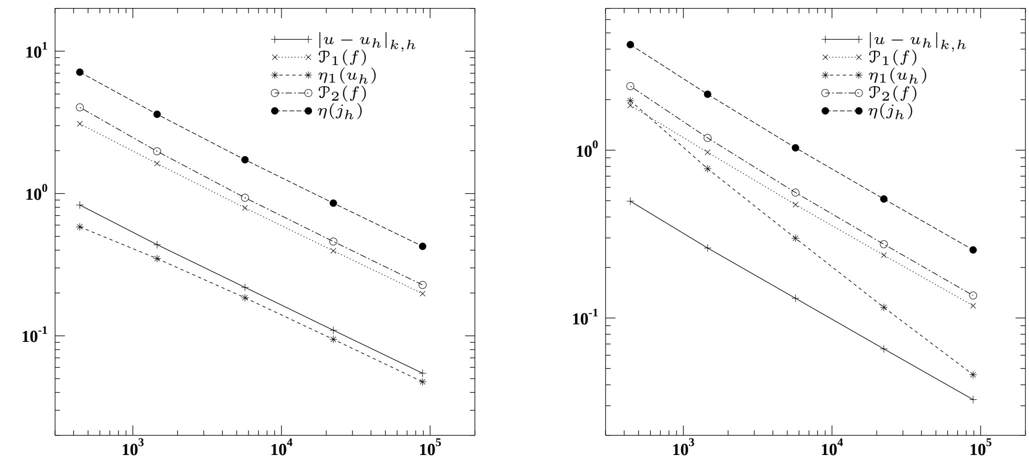

FIGURE 4. Exact error and residual based error indicators as a function of the number of edges in the mesh; left: mildly varying case; right: strongly varying case

Figure 5 presents the same hierarchical error estimators as those considered in figure 3. The same conclusions as for the residual based estimators may be drawn. Our results show in particular that for the present test cases, the saturation constant β does not depend on the ratio $k_{\max}/k_{\min}$.

6. Conclusions

In this paper we have presented a mathematical analysis of various a posteriori error estimates for nonconforming mixed finite element approximations to elliptic problems with variable coefficients. Particular attention was devoted to obtaining upper and lower bounds for the numerical errors valid for strongly heterogeneous media, such as those encountered in applications dealing with subsurface flows. Two types of error estimators were investigated based on either local residual evaluations or on a hierarchical setting using higher-order polynomials (conforming edge bubbles or nonconforming element bubbles). Our numerical results involving test cases with constant, mildly varying and strongly varying coefficients, confirm that all the estimators derived mathematically retain their usefulness in our numerical applications. Since these estimators may be localized at the mesh cells, they may be used to refine the mesh adaptively. Engineering applications with adaptive mesh refinement will be investigated in forthcoming work.

Acknowledgement. The authors are thankful to C. Bernardi (Université Paris VI, France) and J.-P. Croisille (Université de Metz, France) for fruitful discussions.

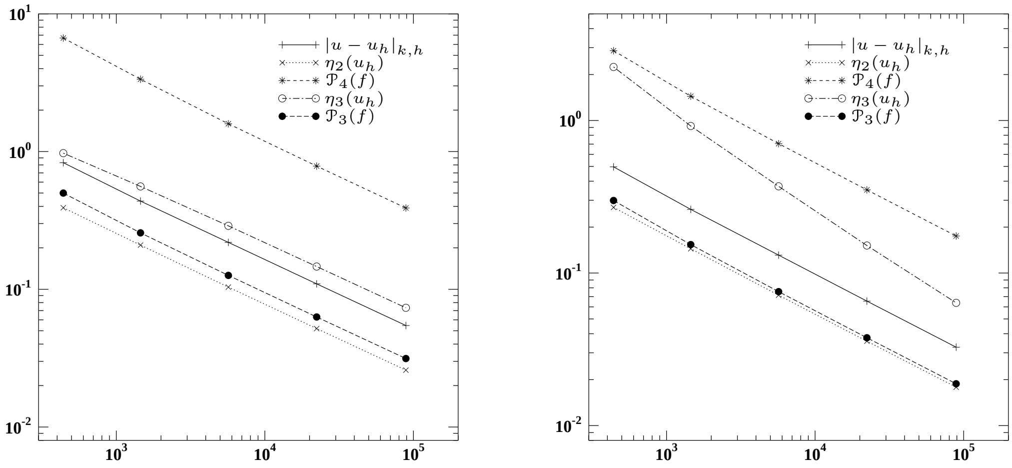

FIGURE 5. Hierarchical error indicators as a function of the number of edges in the mesh; left: mildly varying case; right: strongly varying case

REFERENCES

[1] B. Achchab, S. Achchab, and A. Agouzal. Hierarchical robust a posteriori error estimator for a singularly pertubed problem. *C.R Acad. Paris*, I(336):95–100, 2003.

[2] B. Achchab, A. Agouzal, J. Baranger, and J.F. Maitre. Estimateur d'erreur a posteriori hiérarchique. Application aux éléments finis mixtes. *Numer. Math.*, 80:159–179, 1998.

[3] Y. Achdou and C. Bernardi. Un schéma de volumes ou éléments finis adaptatif pour les équations de Darcy à perméabilité variable. *C.R Acad. Paris*, 2001.

[4] Y. Achdou, C. Bernardi, and F. Coquel. A priori and a posteriori analysis of finite volume discretizations of Darcy's equations. *Numer. Math.*, 2003. in press.

[5] M. Ainsworth and J.T. Oden. *A posteriori error estimation in finite element analysis.* Wiley-Interscience Publication, 2000.

[6] L. Angermann. A posteriori error estimates for FEM with violated Galerkin orthogonality. *Numer. Methods Partial Differ. Equations*, 18(2):241–259, 2002.

[7] I. Babuška and W.C. Rheinboldt. A posteriori error estimates for the finite element method. *Int. J. Num. Meth. Engrg.*, 12:1597–1615, 1978.

[8] R. Bank and K. Smith. A posteriori estimates based on hierarchical bases. *SIAM, J. Numer. Anal.*, 30(4):921–935, 1993.

[9] R.E Bank and A. Weiser. Some a posteriori error estimators for elliptic partial differential equations. *Math. Comp.*, 1985.

[10] C. Bernardi and R. Verfürth. Adaptive finite element methods for elliptic equations with non-smooth coefficients. *Numer. Math.*, 85(4):579–608, 2000.

[11] D. Braess. *Finite elements.* Cambridge Univ. Press, 1997.

[12] B. Courbet and J-P Croisille. Finite volume box schemes on triangular meshes. *Mathematical Modelling and Numerical Analysis*, 32(5):631–649, june 1998.

[13] J.-P. Croisille. Finite volume box schemes and mixed methods. *Math. Mod. Numer. Anal.*, 31(5):1087–1106, 2000.

[14] J-P Croisille and I. Greff. Some nonconforming mixed box schemes for elliptic problems. *Numer. Methods Partial Differ. Equations*, 8(3):355–373, 2002.

[15] A. Ern and J.L Guermond. *Eléments finis : théorie, applications, mise en œuvre*, volume 36 of *SMAI Mathématiques & Applications*. Springer, Heidelberg, 2002.

[16] R.H.W. Hoppe and B. Wohlmuth. Element-oriented and edge-oriented local error estimators for non-conforming finite element methods. *Math. Mod. Numer. Anal.*, 1996.

[17] G. Kanschat and F.T. Suttmeier. A posteriori error estimates for nonconforming finite element schemes. *Calcolo*, 36:129–141, 1999.

[18] F. Schieweck. Upper and lower a posteriori error estimates with post-processing for non-conforming finite elements. Technical report, Magdeburg University, 2001.

[19] R. Verfürth. *A review of a posteriori error estimation and adaptative mesh-refinement techniques.* Chichester, England, 1996.

[20] B.I. Wohlmuth and H.W. Hoppe. A comparison of a posteriori error estimators for mixed finite element discretizations by Raviart-Thomas. *Math. Comp.*, 68(228):1347–1378, 1999.